Powder Technology 241 (2013) 67–73

Contents lists available at SciVerse ScienceDirect

Powder Technology

journal homepage: www.elsevier.com/locate/powtec

Combustion characteristics of high-energy Al/CuO composite powders: The role of oxidizer structure and pellet density

Ji Young Ahn [a], Ji Hoon Kim [a], Jong Man Kim [a,b], Deug Woo Lee [a,b], Jong Kweon Park [c], Donggeun Lee [d], Soo Hyung Kim [a,b,*]

[a] Department of Nano Fusion Technology, College of Nanoscience and Nanotechnology, Pusan National University, San 30 Jangjeon-dong, Geumjeong-gu, Busan 609-735, Republic of Korea
[b] Department of Nanomechatronics Engineering, College of Nanoscience and Nanotechnology, Pusan National University, San 30 Jangjeon-dong, Geumjeong-gu, Busan 609-735, Republic of Korea
[c] Nano Convergence and Manufacturing Systems Research Division, Korea Institute of Machinery and Materials, 171 Jang-dong, Yuseong-gu, Daejeon 305-343, Republic of Korea
[d] School of Mechanical Engineering, Pusan National University, San 30 Jangjeon-dong, Geumjeong-gu, Busan 609-735, Republic of Korea

ARTICLE INFO

Article history:
Received 31 October 2012
Received in revised form 5 March 2013
Accepted 9 March 2013
Available online 15 March 2013

Keywords:
Microparticles
Nanoparticles
Nanowires
Oxidizers
Energetic materials

ABSTRACT

The size and morphology of the fuel and oxidizer and the pellet density are important factors influencing the burn characteristics of energetic-material (EM) pellets. Here, we demonstrate that designed structures of energetic oxidizers with various interfacial contact areas for fuel nanoparticles (NPs) can enhance the explosive reactivities of ignited EM pellets. The measured burn rates and pressurization rates for specific samples of Al NP/porous CuO nanowire (NW) composite pellets were found to be much higher than those for Al NP/CuO NP and Al NP/CuO microparticle (MP) composite pellets. In addition, the explosive reactivities of the EM pellets decreased linearly with increasing pellet density for all compositions of Al NPs/CuO MPs, Al NPs/CuO NPs, and Al NPs/CuO NWs. This suggests that the size and morphology of the oxidizer structures (from solid MPs to porous NWs) and the pellet density of the resulting EM pellets have a synergistic effect, significantly changing the interfacial contact area with the fuel NPs so that the explosive reactivity of the resulting EM pellets can be controlled precisely.

1. Introduction

Energetic materials (EMs) are generally composed of a fuel and an oxidizer, and can generate thermal energy rapidly when they are ignited. The energy release rate of an EM is strongly dependent on various characteristics, including the size, morphology, and chemical composition of the fuel and oxidizer and the magnitude of the interconnections between the fuel and oxidizer. When an EM is ignited by an external energy input such as an electrically heated coil, laser beam, or flame, a so-called self-sustaining exothermic reaction occurs. Those EMs with strong exothermic characteristics can be applied in various engineering fields, for example, for use as explosives, as propulsion fuels, and in pyrotechnics [1–5].

Among various forms of EMs, loose powders composed of micro- or nano-sized reacting fuel and oxidizer particles are being studied widely [6–8]. For the enhancement of the applicability of powder-type EMs, various pellet-type EMs have been fabricated. Pellet-type EMs have the advantages of easy handling and a compact volume for a given mass (i.e., high packing density) compared with loose powder-type EMs, while also being able to release the desired heat energy when ignited. The characteristics of the exothermic reactions of EM pellets are strongly dependent on the physical size and chemical compositions of the fuel and oxidizer, the degree of interfacial contact between the fuel and oxidizer, and the packing density. In previous studies, many research groups have measured the explosive characteristics of EM pellets by controlling the size of the fuel materials (e.g., Al, Fe, Si) and the packing density [9–11]. The use of nano-sized fuel materials of relatively high purity has been reported to reduce the limitations on the mass transport between the fuel and oxidizer so that the reaction becomes kinetically controlled [6–11]. Although numerous EM pellets with enhanced energy-release rates have been successfully formulated by employing nano-sized fuel materials, the effect of the oxidizer structure on the explosive reactivity of EM pellets has hardly been studied.

In this work, we aimed to carry out a systematic investigation of the effects of the size and morphology of the oxidizer and the packing density of the resulting EM pellets on their explosion characteristics. We specifically considered various thermite mixtures of aluminum nanoparticles (Al NPs; fuel) and copper oxide (CuO; oxidizer) of different sizes and morphologies (microparticles (MPs), nanoparticles (NPs), and nanowires (NWs)). We demonstrate that the burn rates and pressurization rates of EM pellets can be controlled simply by perturbing the sizes and morphologies of the oxidizers and varying the packing density of the resulting EM pellets.

* Corresponding author at: Department of Nano Fusion Technology, College of Nanoscience and Nanotechnology, Pusan National University, San 30 Jangjeon-dong, Geumjeong-gu, Busan 609-735, Republic of Korea. Tel.: +82 55 350 5287; fax: +82 55 350 5279.
E-mail address: sookim@pusan.ac.kr (S.H. Kim).

0032-5910/$ – see front matter © 2013 Elsevier B.V. All rights reserved.
http://dx.doi.org/10.1016/j.powtec.2013.03.017

2. Experimental

The commercially available, passivated Al NPs (NT base, Inc.) used as the fuel source in this study had an average primary particle size of 81 ± 4 nm and an oxide layer thickness of approximately 4 nm. The commercially available CuO MPs (Sigma Aldrich) and NPs (NT base, Inc.) used as the oxidizer had average sizes of approximately 6.73 ± 0.36 μm and 98 ± 5 nm, respectively. CuO NWs were fabricated in this study through a combination of electrospinning and calcination processes, which are described in detail elsewhere [12]. Briefly, a polyvinylpyrrolidone (PVP)/copper nitrate ($Cu(NO_3)_2$) precursor solution was prepared by mixing PVP (4 g, Sigma Aldrich, M_w = 55,000) dissolved in ethanol (6 g) with $Cu(NO_3)_2$ (4 g, Sigma Aldrich) dissolved in deionized water (4 g). The PVP/$Cu(NO_3)_2$ precursor solution was then sonicated with ultrasonic energy (200 W, 40 kHz) for 1 h. After sonication, the PVP/$Cu(NO_3)_2$ precursor solution was dispensed at a rate of 0.75 mL/h using a precision syringe pump (model no. 781100, KD Scientific). While dispensing the precursor solution, a fixed positive voltage of approximately 35 kV was applied to the tip of the syringe nozzle, while the iron mesh covering the rotating plate was simultaneously grounded. Here, the distance between the nozzle tip and the rotating plate was fixed at 15 cm. Subsequently, PVP/$Cu(NO_3)_2$ composite NWs were formed through Coulombic explosion, and were deposited on the surface of the iron mesh. These PVP/$Cu(NO_3)_2$ composite NWs were then calcined at 400 °C for 3 h in a tube furnace to remove the polymer template (PVP) and simultaneously convert the $Cu(NO_3)_2$ into CuO NWs by thermal decomposition.

EM pellets were then fabricated by applying various normal forces on the EM powders, which were composed of different mixtures of Al NPs/CuO MPs, Al NPs/CuO NPs, and Al NPs/CuO NWs, as shown in the schematic of Fig. 1. Briefly, Al NPs (fuel) were mixed with CuO MPs/NPs/NWs (oxidizer) in EtOH solution. The mixing ratio between the fuel and oxidizer was fixed at Al:CuO = 30:70 wt.%. The Al/CuO in EtOH solution was then sonicated under a power of 200 W and frequency of 40 kHz for 5 min to achieve homogeneous mixing. Then, the EtOH was evaporated at 80 °C in a convection oven for 30 min. The resulting EM powder (26 mg) was pressed into a disc-shaped pellet with a diameter of 8 mm using a homemade uniaxial press, by applying various forces in the range 4905–19,620 N for 10 min. The thickness of the EM pellets was varied to obtain the desired % theoretical density (%TD) (or packing density), which indirectly represents the magnitude of the pressing force on the EM powders. The %TD values were calculated by taking the ratios of the real bulk density to the theoretical density of the composites. Here, the theoretical density (D) of a composite with two components is defined as follows:

$$D = (W_1 + W_2)/(W_1/D_1 + W_2/D_2) \quad (1)$$

where W_1 is the mass ratio of Al (=0.3), W_2 is the mass ratio of CuO (=0.7), D_1 is the bulk density of Al (=2.7 g/cm^3), and D_2 is the bulk density of CuO (=6.3 g/cm^3). On the basis of Eq. (1), the resulting theoretical density of the Al/CuO composite was calculated to be approximately 4.5 g/cm^3. Therefore, the resulting Al/CuO-based loose EM powder was determined to be approximately 38%TD, and the Al/CuO-based EM pellets pressed by various forces in this approach were determined to range from 45%TD (i.e., weakest press of 4905 N) to 80%TD (i.e., strongest press of 19,620 N).

The morphologies of the EM powders and pellets were characterized using a scanning electron microscope (SEM; Model S4700, Hitachi) operated at 15 kV and a transmission electron microscope (TEM; Model JEM-2100, JEOL) operated at 200 kV. In order to observe the explosion characteristics of the different types of EM powders and pellets, we measured the burn rates and pressurization rates. After flame ignition, the burn rates of the EM powders and pellets were monitored using a high-speed camera (Model SR-Ultra-C, Kodak). In addition, the pressurization rates of the EM powders and pellets were measured using a pressure cell test (PCT) system [8,12]. Briefly, the prepared EM powders and pellets were placed in the reaction vessel (13 mL) and ignited using a heated tungsten wire with a direct current of 2 A at 1.5 V. The explosion-induced pressurization rate was measured in situ using the pressure sensor system. The initial signal measured by the pressure sensor (model no. 113A03, PCB Piezotronics, maximum detection range of 120 psi) was then amplified by an in-line charge amplifier (Model No. 422E11, PCB Piezotronics). The signal was transformed into a voltage output at the sensor signal conditioner (Model No. 480C02, PCB Piezotronics). This voltage output was then recorded by a digital oscilloscope (TDS 2012B, Tektronix).

3. Results and discussion

Three different EM pellets were prepared with Al NPs/CuO MPs, Al NPs/CuO NPs, and Al NPs/CuO NWs. The average diameter of the

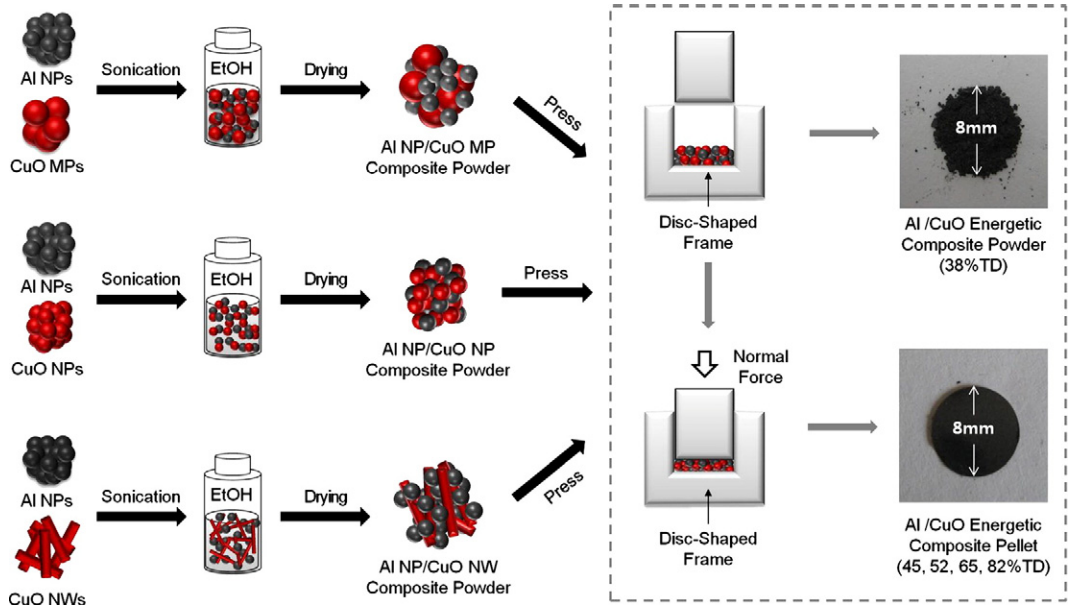

Fig. 1. Schematic of the experimental process for generating EM pellets composed of Al NP/CuO MP, Al NP/CuO NP, and Al NP/CuO NW composites.

spherical primary Al NPs as the fuel was 81 ± 4 nm, and the thickness of the oxide layer was approximately 4 nm, as shown in Fig. 2a and b. The average diameters of the primary CuO MPs and CuO NPs were 6.73 ± 0.36 μm and 98 ± 5 nm, respectively, as shown in Fig. 2c, d, e, and f. The CuO NWs were found to have an average diameter of 213 ± 4 nm and an average length of 11.5 ± 0.8 μm, as shown in Fig. 2g, and they also had highly porous structures inside, as shown in Fig. 2h.

The fuel and oxidizer powders were then mixed and pressed with various normal forces to form EM pellets. The SEM and TEM analyses show that irregular, blunt CuO MPs combined with spherical Al NPs were observed for the Al NP/CuO MP-based EM powders, as shown in Fig. 3a and d. In the case of Al NP/CuO NP-based EM powders, as shown in Fig. 3b and e, both spherical Al NPs and spherical CuO NPs were closely connected with each other. In the case of Al NP/CuO NW-based EM powders, as shown in Fig. 3c and f, highly porous CuO NWs were observed to connect closely with the spherical Al NPs. After the pressing of each of the EM powders with a force of 9810 N, the surfaces of the EM pellets were observed using the SEM. For the Al NP/CuO MP-based EM pellet, rough surface structures with an inhomogeneous distribution and large pores between the Al and CuO components were clearly observed, as shown in Fig. 3g. However, the surfaces of the Al NP/CuO NP- and Al NP/CuO NW-based pellets were observed to have relatively homogeneous distributions and smaller pores between the Al and CuO components, as shown in Fig. 3h and i. This suggests that the degree of homogeneous intermixing between the Al and CuO

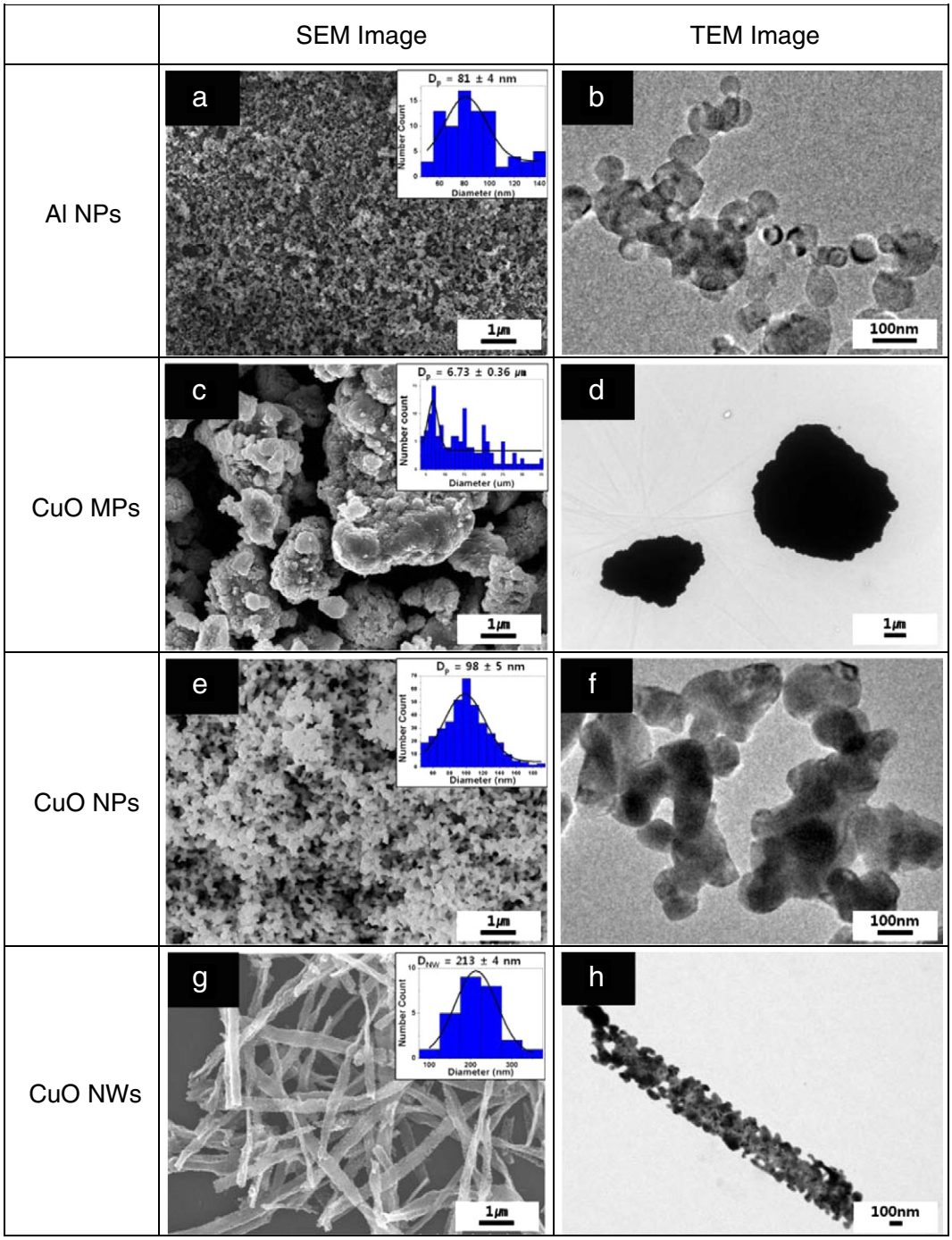

Fig. 2. SEM and TEM images of (a, b) Al NPs, (c, d) CuO MPs, (e, f) CuO NPs, and (g, h) CuO NWs. (The insets are the particle size distributions; D_p is the average particle size, and D_{NW} is the average nanowire diameter.)

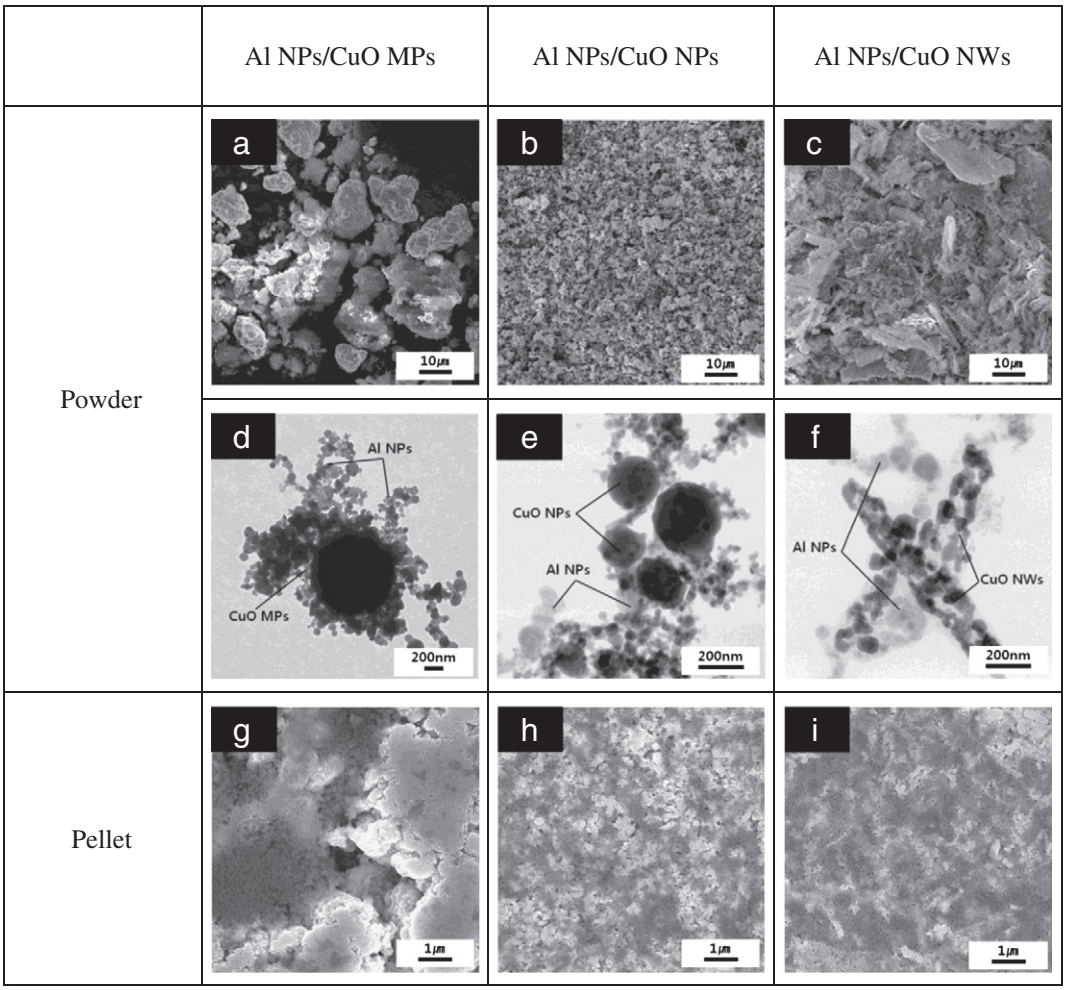

Fig. 3. SEM and TEM images of (a, d) Al NP/CuO MP composite powder, (b, e) Al NP/CuO NP composite powder, and (c, f) Al NP/CuO NW composite powder. SEM images of the surface of (g) Al NP/CuO MP, (h) Al NP/CuO NP, and (i) Al NP/CuO NW composite pellets.

components can be enhanced by employing uniform nano-sized reactants with a higher interfacial contact area.

The presence of Al and CuO crystallites in the micro- and nano-structures employed in this study was examined by XRD analysis, as shown in Fig. 4a. The XRD spectra showed very strong diffractions from the Al NPs, CuO MPs, CuO NPs, and CuO NWs, suggesting that pure Al and CuO powders as the sources of reacting materials were used to form the Al/CuO-based EM powders and pellets. After ignition, the completeness of the exothermic reaction of the Al/CuO composite pellets was also examined by performing XRD analysis. The results are shown in Fig. 4b; the signals of Al and CuO disappeared, and strong signals of Al_2O_3 and Cu appeared, suggesting that the redox reaction between Al and CuO was completed using this approach (i.e., $2Al + 3CuO \rightarrow Al_2O_3 + 3Cu$; heat of reaction $= -1212.5$ kJ/mol [13]).

The effects of the size and morphology of the oxidizer on the explosion characteristics of the EM composites were examined by monitoring the flame propagation speed of the ignited EM powders using a high-speed camera. Fig. 5 shows a series of snapshots of the flame propagation of ignited EM powders. The total time taken for the explosive reaction was found to be approximately 70, 22, and 9 ms for the Al NP/CuO MP, Al NP/CuO NP, and Al NP/CuO NW composite powders, respectively. The burn rates of the Al NP/CuO MP, Al NP/CuO NP, and Al NP/CuO NW composite powders were then determined to be approximately 6, 80, and 120 m/s, respectively. This suggests that a smaller size and higher contact area of the oxidizer structure for the given nano-sized fuel NPs strongly promoted the exothermic reaction of the resulting EM composites. This is presumably because oxygen was rapidly provided from the neighboring oxidizer, which was in close proximity with the fuel, when the EM composites were ignited. Here, although the CuO NWs had a larger average diameter than the CuO NPs, the burn rate of the Al NP/CuO NW-based EM powders (i.e., 120 m/s) was found to be almost 1.5 times faster than that of the Al NP/CuO NP-based EM powders (i.e., 80 m/s). This is presumed because CuO NWs have highly porous structures inside, so there is a relatively high interfacial contact area between the Al NPs and CuO NWs (see Fig. 3f). This was also corroborated by nitrogen gas adsorption analysis (i.e., Brunauer–Emmett–Teller (BET) analysis) for the CuO NPs and NWs. The specific surface areas determined by BET analysis were ~5 and ~90 m^2/g for the CuO NPs and CuO NWs, respectively.

The effects of the size and morphology of the oxidizers on the burn rate of EM composites with various pellet densities are presented in Fig. 6. The burn rates of the three different Al/CuO composite pellets decreased with increasing pellet density. A more rapid drop-off in burn rate at relatively low pellet densities (38–52%TD) and then a gradual decrease in burn rate at higher pellet densities (52–82%TD) were generally observed for all the EM pellets. This is presumably because the increased heat dissipation in EM pellets with higher pellet densities could suppress the propagation of the burn front to some extent. In addition, the possible damages of oxide shell of Al NPs made by pressing the EM powders could significantly reduce the pressure inside the molten Al, which accordingly results in suppressing the dispersion of liquid-like Al clusters for fast reaction with

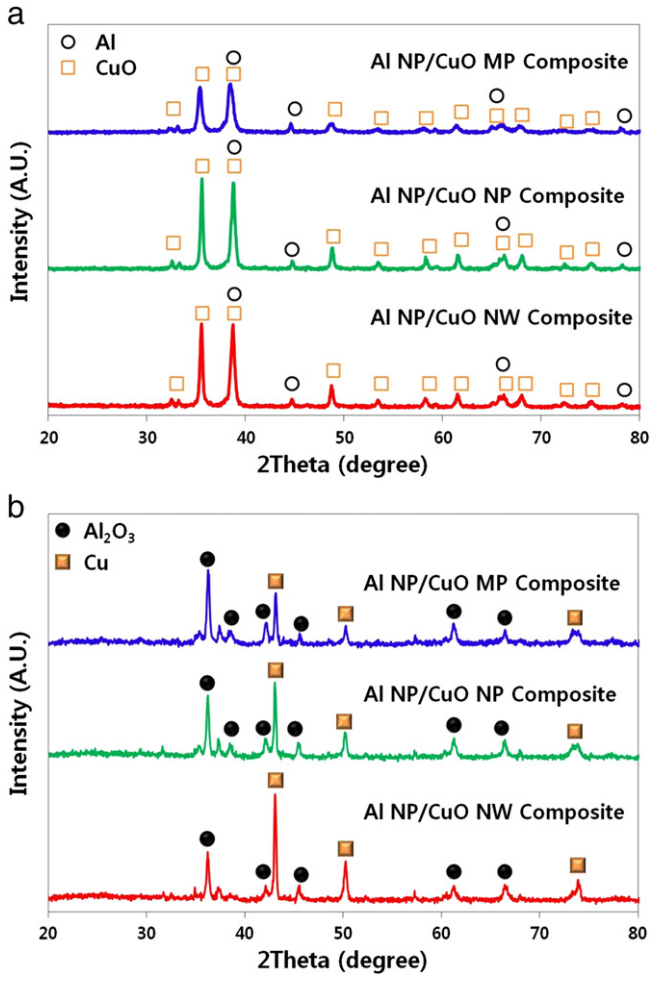

Fig. 4. XRD signals of Al NP/CuO MP, Al NP/CuO NP, and Al NP/CuO NW composite pellets (a) before flame-ignition test and (b) after flame-ignition test.

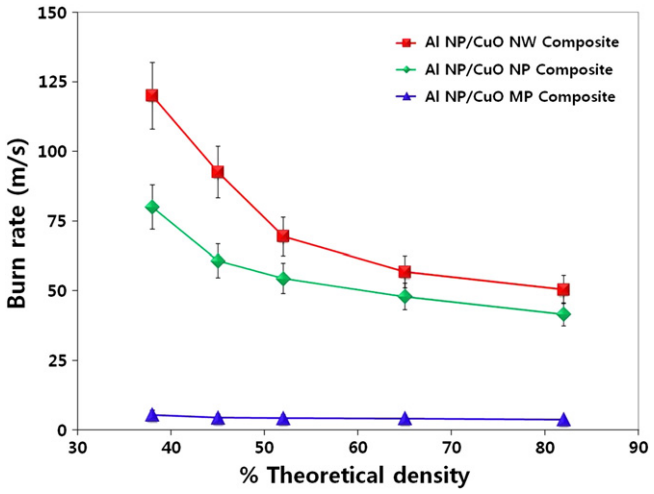

Fig. 6. Burn rates of various Al/CuO composite pellets as a function of size and morphology of oxidizer and pellet density.

oxidizers when EM pellets are ignited [14]. The relative burn rates were determined to be in the order Al NPs/CuO NWs > Al NPs/CuO NPs > Al NPs/CuO MPs for all the %TD ranges considered in this approach. A higher interfacial contact area in the Al NP/CuO NW and Al NP/CuO NP composite pellets results in a relatively faster burn rate. Another possible reason for the much slower burn rate of the Al NP/CuO MP composite pellets could be the presence of large pores and an inhomogeneous distribution between the Al NPs and CuO MPs in the EM pellet (Fig. 3a and g). This suggests that oxidizer nanostructures with higher interfacial contact areas for the given fuel NPs promote the burn rate of EM pellets, and simultaneously, the pellet density of the EM pellets also plays a key role in controlling the burn characteristics.

A fixed mass of the various EM pellets (26 mg) was ignited in the PCT system, and the pressurization rate of the confined reaction cell corresponding to the ignition of the EM pellets was measured in situ. Fig. 7a, b, and c presents the pressure traces of the ignited EM pellets formed with various pellet densities. One can easily see that the Al NP/CuO NW composite pellets showed the highest pressurization rates for all the pellet densities considered. The magnitude of the maximum pressure was then decreased and the rise time was slowed upon subsequent employment of Al NP/CuO NP and Al NP/CuO MP composite pellets for all the pellet densities. Fig. 7d summarizes the

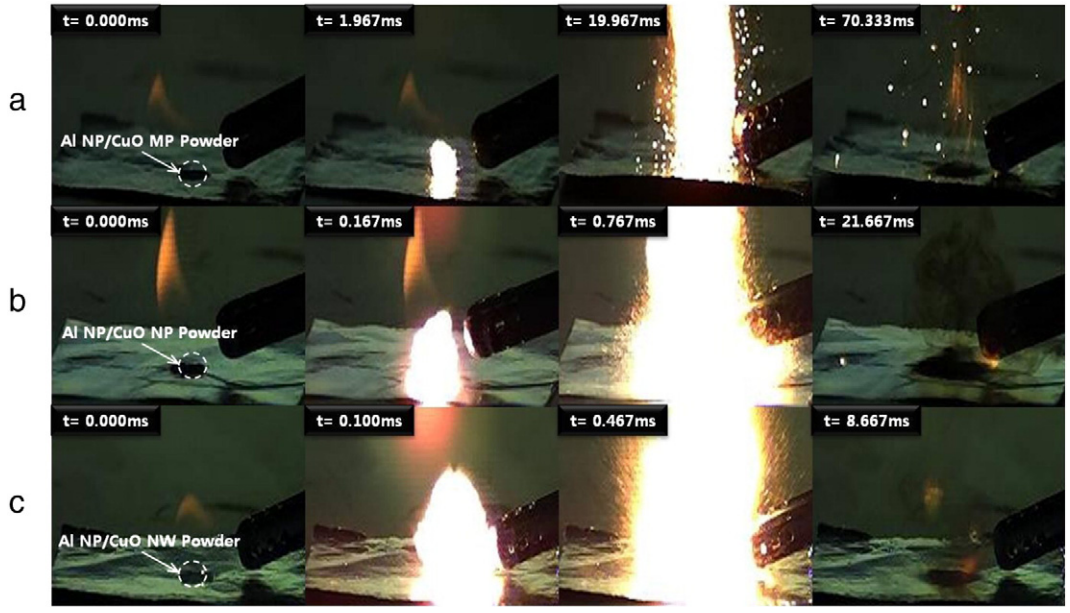

Fig. 5. Snapshots of flame-ignited (a) Al NP/CuO MP composite powder, (b) Al NP/CuO NP composite powder, and (c) Al NP/CuO NW composite powder.

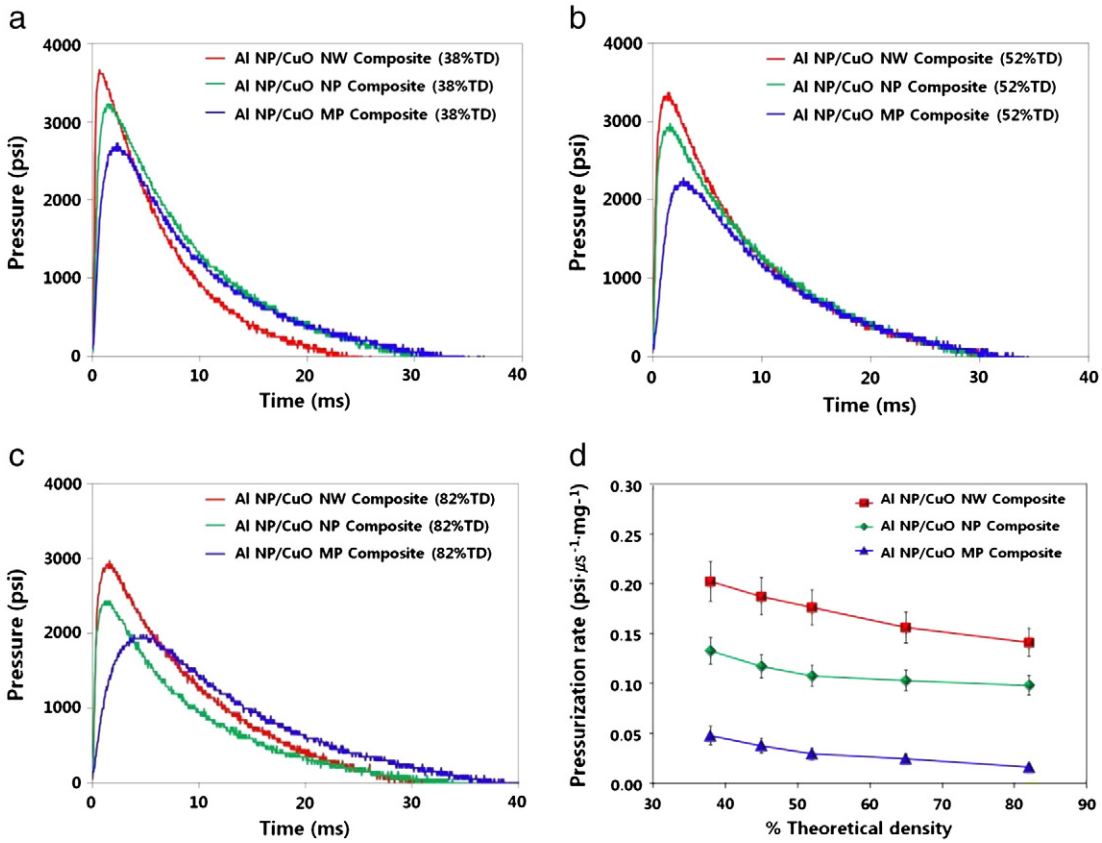

Fig. 7. Pressure traces of ignited EM pellets with different oxidizer structures and pellet densities of (a) 38%TD, (b) 52%TD, and (c) 82%TD. (d) Pressurization rates of various EM pellets as a function of pellet density.

pressurization rates of the 26 mg samples of the various EM pellets as a function of pellet density. Here, the pressurization rate was determined by taking the ratio of the maximum pressure to the rise time. The pressurization rates of the Al NP/CuO NW, Al NP/CuO NP, and Al NP/CuO MP powders were observed to be approximately 0.21, 0.14, and 0.05 $psi \cdot \mu s^{-1} \cdot mg^{-1}$, respectively, for the case of 38%TD, and decreased significantly to 0.15, 0.10, and 0.02 $psi \cdot \mu s^{-1} \cdot mg^{-1}$, respectively, for the case of 82%TD pellets. Thus, as the pellet density increased, the pressurization rate of the 26 mg samples of the EM pellets decreased significantly. It is interesting to note that the evolution of the pressurization rate of EM pellets as a function of pellet density is very similar to that of the burn rate of EM pellets (see Figs. 6 and 7d). We believe that both the burn rate and pressurization rate are strongly correlated with the explosion reactivity of EM powders and pellets. Therefore, the pressurization rates of EM pellets with higher pellet densities are accordingly reduced by increased thermal losses through heat transfer. This is presumably due to the compact bonding between the reacting materials, which, in turn, eventually quenches the propagation of the explosion reactivity in the EM pellets.

4. Conclusions

We have demonstrated that the size and morphology of the CuO oxidizer have strong effects on the explosion reactivity of the resulting high-energy Al/CuO composite powders and pellets. The designed structures of energetic oxidizers, which provide higher interfacial contact areas for the fuel NPs, can significantly promote the resulting explosion reactivity of ignited EM pellets through the rapid supply of oxygen from the oxidizers, which are located close to the fuel metals. Another dominating factor influencing the burn characteristics of EM pellets is the pellet density. As the pellet density of Al NP/CuO MP, Al NP/CuO NP, and Al NP/CuO NW composite pellets increases, the accordingly increased thermal losses by heat transfer due to the stronger bonding between the Al and CuO components can suppress the propagation of the burn front in the EM pellets, so the resulting burn rate and pressurization rate of the ignited EM pellets are reduced significantly. Through the creation of a suitable energetic oxidizer nanostructure and the adjustment of pellet density of the resulting EM pellets, EM composite powders and pellets with the desired explosive reactivity can be obtained.

Acknowledgments

This work was supported by the Global Frontier R&D Program on Center for Multiscale Energy System funded by the National Research Foundation under the Ministry of Education, Science and Technology, Korea (2012M3A6A7054863). This work was also partially supported by the “Development of next-generation multifunctional machining systems for eco/bio components” project of the Ministry of Knowledge Economy.

References

[1] J.J. Granier, M.L. Pantoya, Combustion and Flame 138 (2004) 378.
[2] K. Zhang, C. Rossi, M. Petrantoni, N. Mauran, Journal of Microelectromechanical Systems 17 (2008) 832.
[3] R.A. Guidotti, P. Masset, Journal of Power Sources 161 (2006) 1443.
[4] S.F. Son, Materials Research Society Symposium Proceedings 800 (2004) AA5.2.
[5] M. Petrantoni, C. Rossi, L. Salvagnac, V. Conedera, A. Esteve, C. Tenailleau, P. Alphonse, Y.J. Chabal, Journal of Applied Physics 108 (2010) 084323.
[6] S.H. Kim, M.R. Zachariah, Advanced Materials 16 (20) (2004) 1821.
[7] A. Prakash, A.V. McCormick, M.R. Zachariah, Nano Letters 5 (2005) 1357.
[8] C. Rossi, A. Esteve, P. Vashishta, Journal of Physics and Chemistry of Solids 71 (2010) 57.

[9] J.J. Granier, M.L. Pantoya, Materials Research Society Symposium Proceedings 800 (2004) 173.
[10] J.W. Reed, R.R. Walters, R.A. Guidotti, A.K. Jacobson, IEEE 35th Power Sources Symp. Proc., 211, 1992.
[11] R.A. Guidotti, J. Odinek, F.W. Reinhardt, Journal of Energetic Materials 24 (2006) 271.
[12] J.Y. Ahn, W.D. Kim, K. Cho, D.G. Lee, S.H. Kim, Powder Technology 211 (2011) 65.
[13] J.L. Cheng, H.H. Hng, H.Y. Ng, P.C. Soon, Y.W. Lee, Journal of Physics and Chemistry of Solids 71 (2) (2010) 90.
[14] V.I. Levitas, B.W. Asay, S.F. Son, M.L. Pantoya, Applied Physics Letters 89 (7) (2006) 071909.